Available online at www.sciencedirect.com
ScienceDirect
Trans. Nonferrous Met. Soc. China 25(2015) 2499−2508
Transactions of Nonferrous Metals Society of China
www.tnmsc.cn

Optimizing consolidation behavior of Al 7068−TiC nanocomposites using Taguchi statistical analysis

Amin AZIMI[1], Ali SHOKUHFAR[2,3], Omid NEJADSEYFI[2], Hamid FALLAHDOOST[2], Saeid SALEHI[3]

1. Young Researchers and Elite Club, South Tehran Branch, Islamic Azad University, Tehran, Iran;
2. Advanced Materials and Nanotechnology Research Center, Department of Mechanical Engineering, K. N. Toosi University of Technology, Tehran, Iran;
3. Department of Engineering, Karaj Branch, Islamic Azad University, Karaj, Iran

Received 5 October 2014; accepted 10 February 2015

Abstract: The fabrication of high strength Al 7068−5%TiC (mass fraction) nanocomposite was studied by mechanical alloying and hot pressing routes. Considering densification importance and grain growth effects, hot pressing process conditions for producing bulk nanocomposite were optimized using statistical Taguchi method based on compressive strength achievement. The Taguchi results indicate that 30 min hot pressing under pressure of 500 MPa at 385 °C provides high compressive strength and hardness of 938 MPa and HV 265, respectively. More interestingly, analysis of variance proves that the applied pressure is the most influential factor for hot pressing of the nanocomposite. The contribution percentages of factors in hot pressing terms are as follows: applied pressure (61.3%), exposed temperature (29.53%) and dwelling hot pressing time (4.49%).

Key words: Al 7068−TiC nanocomposite; hot pressing; mechanical alloying; Taguchi method; mechanical properties

1 Introduction

Aluminum alloys possess many outstanding attributes that lead to a wide range of aeronautical field applications which require high strength, light mass and energy savings characteristics [1−3]. Al 7068 alloy (Al−7.8%Zn−2.6%Mg−2%Cu−0.1%Zr, mass fraction) is one of the most famous 7xxx series aluminum alloys which can provide high mechanical strength with alloying elements [3,4]. Despite this fact, higher strength is needed in order to replace heavier metals with this alloy in some applications at ambient and elevated temperatures [5]. Using these alloys as matrix composites is known to offer better bulk mechanical properties. There are extensive research experiences in producing composites by nanometric carbides, oxides, nitrides and different intermetallic compounds reinforcement such as Al_2O_3, B_4C and SiC by powder metallurgy [6−9]. TiC was not studied enough for 7xxx Al alloys as reinforcement in nano size scale. Excellent properties of TiC motivated authors to fabricate Al 7068-based nanocomposite. Mechanical alloying using ball milling has been successfully employed to improve the reinforcement of nanoparticle distribution throughout the matrix. Mechanical alloying by repetitive cold-welding, fracturing and dynamic recrystallization mechanism can provide driving force for activated inter-diffusion among the powder particles [10−12]. Uniform distribution of nanometric reinforcement with partial agglomeration was also provided in nanocomposites by mechanical alloying [13,14]. To obtain high-density bulk materials from mechanically alloyed powders, consolidation of particles is intransitive. Although there are different methods to compact powders, hot pressing enables net-shaped and cost-effective processing with controlled microstructure and mechanical properties. Hot pressing method is widely used to consolidate Al matrix nanocomposite powders by simultaneous application of heat and pressure [15−18]. Presence of pressure factor increases interface surface area in particles and subsequently improves sintering condition [19,20]. High-strength bonding between particles can be formed while hot pressing is carried out under optimal conditions of temperature, pressure and time. This can provide high density of bulk sample.

Some valuable studies about prediction and analysis of the influence of processing parameters on the

Corresponding author: Amin AZIMI; Tel: +98-9124808438; Fax: +98-2144603072; E-mail: aminazimi.kntu@gmail.com
DOI: 10.1016/S1003-6326(15)63868-7

synthesis of Al-based nanocomposite were performed by CANAKCI et al [21−24]. The effect of hot pressing parameters on mechanical properties is worthy to be investigated. Although increasing time and temperature improves sintering act, grain growth is more intense in these conditions [25−27]. It is proved that the grain growth phenomenon in nanocrystalline structures decreases the mechanical properties [28]. Also, many investigations are asserted that the density increases with increasing the compaction pressure with a decelerating rate. This means that the pressure is effective below a specified upper limit [20].

There were many researches about the fabrication of consolidated nanostructured Al alloys and Al-based nanocomposite by hot pressing method [15−18,29]. Relative density of 97% was obtained in nanostructured pure Al that was hot pressed under 350 MPa at 450 °C for 1 h in Ref. [15]. TAVOOSI et al [14] observed relative density of 96% for consolidated Al−13.8%Zn (mass fraction) with a crystallite size of 40 nm which could be related to 20 min of hot pressing under 400 MPa at 400 °C. Also, JAFARI et al [16] investigated the effect of temperature and time of hot pressing on the relative density of nanostructured Al 2024 and Al 2024−MWCNT nanocomposites. Relative densities of higher than 98% and slightly lower than 99% were achieved for Al 2024 and Al 2024−1.5%MWCNT (volume fraction), respectively under pressure of 250 MPa of hot pressing at 500 °C for 30 min. ATRIAN et al [17] perceived 97.84% for relative density applying 500 MPa at 425 °C in 30 min for hot pressing of Al7075−5%SiC (volume fraction) nanocomposite.

Taguchi method is a preferable technique to provide optimal reliable information by making fewer possible runs [30,31]. This method is to realize the optimal and robust process characteristics that have a minimized sensitivity to noises [32]. Taguchi recommended signal-to-noise (S/N) ratio as the objective function for matrix experiments. This function is classified into three categories: 1) smaller is better (LB), 2) larger is better (HB) and 3) nominal is best (NB). Therefore, depending on this target, every response datum is converted to ratio of signal to noise (S/N ratio) and the maximum values of S/N ratios are selected as optima values for each parameter [30,33]. To the best of the authors' knowledge, there is no clear research on the finding optimal hot pressing condition for the preparation of Al 7068−TiC nanocomposites.

The present study focused on the optimization of hot pressing parameters for the preparation of Al 7068−TiC nanocomposite using Taguchi experimental design. Considering the previous literature achievements to consolidate nanostructured Al alloy powders, three different parameters were chosen: pressure, temperature and time of hot pressing. The maximum value of compressive strength was evaluated in this research. Moreover, an attempt was taken to study the contribution percentage of each experimental parameter of hot pressing procedure.

2 Experimental

2.1 Materials and fabrication

Commercial powder mixture of Al, Zn, Mg, Cu and Zr was applied to fabricating Al alloy (Al−7.8%Zn−2.6%Mg−2%Cu−0.1%Zr) by powder metallurgy (PM) method. The chemical composition of this alloy is equivalent to Al 7068. The particle size and purity of initial Al 7068 elemental powders are the same as the earlier reported in Ref. [4]. This sample was produced as reference material which is referred as Al 7068-PM in this work. In order to produce Al 7068−TiC nanocomposite, 5% (mass fraction) of nano-sized TiC powders was added to the blended matrix elemental powder before starting mechanical alloying. This sample is referred to as Al 7068−TiC. Figure 1 shows the TEM image of TiC nanoparticles used in this study. As it can be seen, the average size of these particles was about 40 nm. Mechanical alloying was conducted in a planetary high-energy ball mill Fritsch–P6 under argon atmosphere using stainless steel balls with 10 mm in diameter. The milling was continued for 40 h [4]. The mass ratio of ball to powder was approximately 15:1 and the mill speed was maintained at 250 r/min. 0.5% (mass fraction) of stearic acid as process control agent (PCA) was added to retard excessive welding. The microstructures of synthesized alloy matrix and nanocomposite powder samples were characterized by XRD, SEM (Philips XL30) and supplemental EDX. The XRD patterns were recorded in the 2θ range of 20°−100° (step size 0.031°) using a Philips diffractometer (40 kV) with Cu K_α radiation (λ=0.15406 nm), in order to investigate structural changes of alloyed powder.

Subsequently, the obtained powder of Al 7068−TiC was hot-pressed in a self-made cylindrical uniaxial die

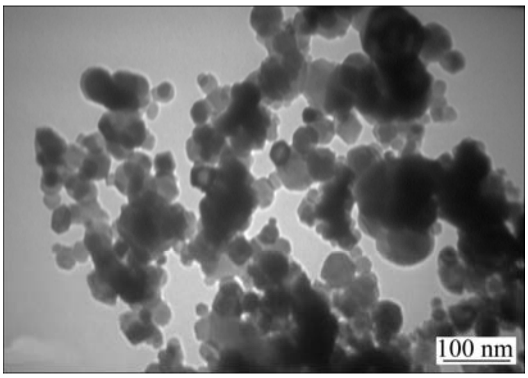

Fig. 1 TEM image of nanometric TiC reinforcement

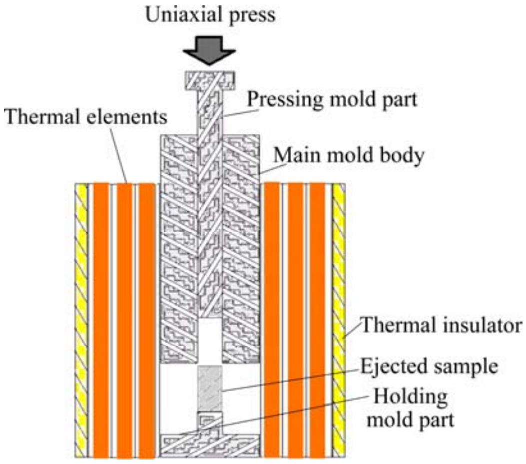

Fig. 2 Schematic section of hot pressing setup

(Fig. 2). Then, they were cooled to ambient temperature and stripped off the die. The output samples with the dimensions of 10 mm in diameter and 15 mm in length were prepared by machining the consolidated powder for the evaluation of mechanical properties. Based on a DSC analysis and related starting point of the endothermic peak at 550 °C (t_m), hot pressing temperatures were chosen as $0.6t_m$, $0.7t_m$ and $0.8t_m$ which were 330, 385 and 440 °C, respectively. The microstructure of consolidated samples was observed using optical microscope (OM). Density values of compact samples were measured using Archimedes and theoretical approaches. Compression experiments at strain rate of 1 mm/s were performed by Instron-type machine (Hounsfield H50−KS model) at ambient temperature according to ASTM E9−89a standard. Teflon sheet was applied in order to minimize the effects of friction between the platen and specimen interface.

2.2 Taguchi method

This study paid attention to three controllable factors, and each factor has three levels which are shown in Table 1. Thus, an L9 orthogonal array was used and the experimental conditions can be attained by combining Table 1 and L9 (3^4) orthogonal array.

Table 1 Controllable hot pressing factors and their levels

Factor	Level 1	Level 2	Level 3
A, pressure/MPa	500	400	300
B, temperature/°C	440	385	330
C, dwelling time/min	45	30	15

The S/N ratio with HB characteristics is required due to obtaining enhanced mechanical properties of the Al 7068 (PM)−TiC nanocomposites. S/N ratio is calculated by

$$\frac{\mathrm{S}}{\mathrm{N}}=-10\lg\left(\frac{1}{n}\sum_{i=1}^{n}\frac{1}{Y_i^2}\right) \tag{1}$$

where n is the number of experiments in a trial, and Y_i represents the result of measurement. The analysis of mean (ANOM) statistical approach was used to obtain the optimum combination of design parameters. Thereby, the mean of the S/N ratio of each controllable factor at a specified level must be calculated in next step. The mean of the S/N ratio of factor I at level i, $(M)_{\mathrm{Factor}=I}^{\mathrm{Level}=i}$ is achieved by the following formula:

$$(M)_{\mathrm{Factor}=I}^{\mathrm{Level}=i}=\frac{1}{n_{Ii}}\sum_{j=1}^{n_{Ii}}\left[\left(\frac{\mathrm{S}}{\mathrm{N}}\right)_{\mathrm{Factor}=I}^{\mathrm{Level}=i}\right]_j \tag{2}$$

where n_{Ii} indicates the number of appearances of factor I at level i and $\left(\frac{\mathrm{S}}{\mathrm{N}}\right)_{\mathrm{Factor}=I}^{\mathrm{Level}=i}$ represents the S/N ratio of factor I at level i.

The analysis of variance (ANOVA) statistical procedure was applied to determining the contribution percentage of each controllable factor, ρ_{F}, on the densification and mechanical properties of the Al alloy, which is calculated using the following equation:

$$\rho_{\mathrm{F}}=\frac{\mathrm{SS_F}-(\mathrm{DOF_F}V_{\mathrm{Er}})}{\mathrm{SS_T}}\times 100 \tag{3}$$

where $\mathrm{DOF_F}$ represents the degree of freedom for each factor which is obtained by subtracting one from the number of the levels for each factor. The total sum of squares, $\mathrm{SS_T}$, is also practically determined as

$$\mathrm{SS_T}=\sum_{j=1}^{m}\left(\sum_{i=1}^{n}Y_i^2\right)-mn\overline{Y}_{\mathrm{T}}^{\,2} \tag{4}$$

where

$$\overline{Y}_{\mathrm{T}}=\sum_{j=1}^{m}\left(\sum_{i=1}^{n}Y_i\right)/(mn) \tag{5}$$

In Eqs. (4) and (5), m reveals the number of performed experiments and n indicates the number of repetitions of same experimental conditions. The factorial sum of squares, $\mathrm{SS_F}$, is given by

$$\mathrm{SS_F}=\frac{mn}{L}\sum_{k=1}^{L}\left(\overline{Y}_k^{\mathrm{F}}-\overline{Y}_{\mathrm{T}}\right)^2 \tag{6}$$

where $\overline{Y}_k^{\mathrm{F}}$ indicates the average value of the measurement results of a certain factor in the kth level. The variance of error, V_{Er}, is achieved by the following mathematic relation:

$$V_{\mathrm{Er}}=\frac{\mathrm{SS_T}-\sum_{\mathrm{F}=A}^{D}\mathrm{SS_F}}{m(n-1)} \tag{7}$$

3 Results and discussion

3.1 Characterization of powder samples

Figure 3 shows powder morphology variations during the mechanical alloying. As a result of severe plastic deformation, particles are flake-like at 15 h of milling. Gradually, the morphology of powder particles was changed from flake-like to spherical when the milling time was extended to 30 h. It is proved that spherical powders have a lower tendency to form bridges, and because of the relatively good mobility, pack quite densely [34]. In this stage, plastic deformation and cold welding are more dominant than fracturing. With further milling up to 40 h, the particle size was decreased due to the fact that fracturing was dominated in the powder particles. Work hardening during milling resulted in continuous refinement of matrix powder particles [13]. It should be noted that the decrease of the particle size can affect the properties of nanocomposite [35,36].

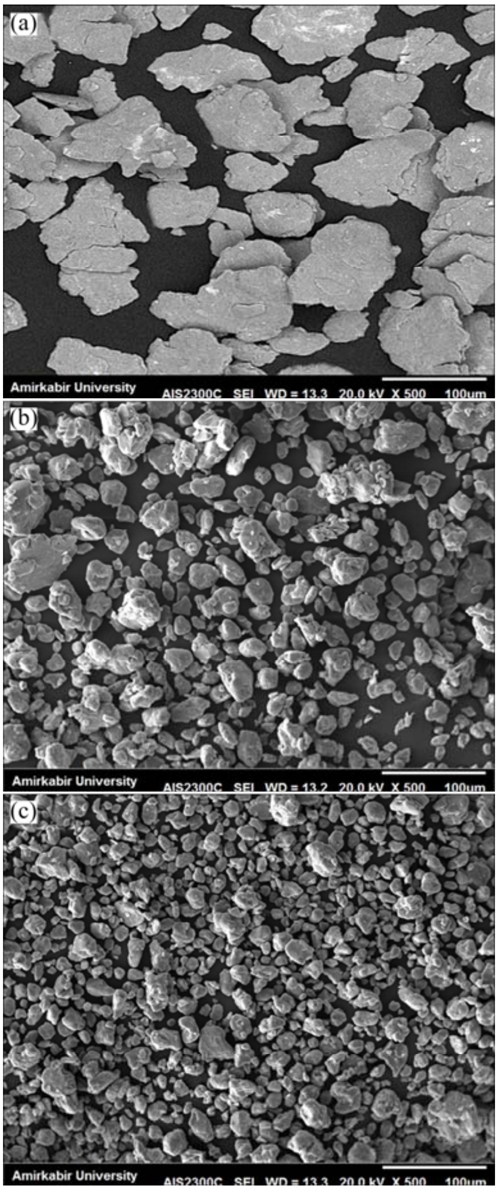

Fig. 3 Variations in morphology of particles after different time of milling: (a) 15 h; (b) 30 h; (c) 40 h

In order to precisely investigate some common impurities in the milled powders, analysis of EDX was performed in the obtained powders. Figure 4 represents EDX spectra of the 40 h-milled nanocomposite powder. As expected, the Al 7068 elemental alloy and TiC reinforce component in the powder were identified. In addition, Fe peak is also visible as an inevitable impurity of mechanical alloying process. However, so small an amount of unintentionally added Fe was about 0.2%, which is not considerable.

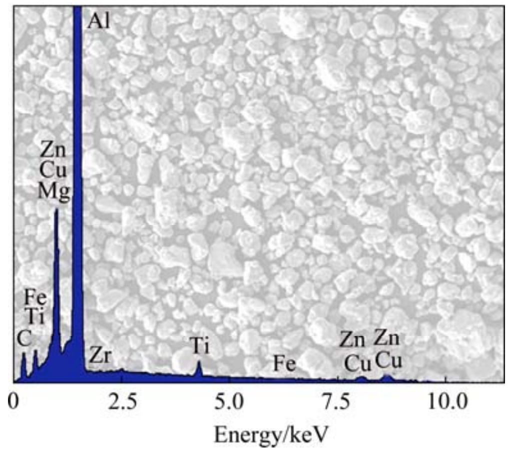

Fig. 4 EDX spectrum of 40 h-milled sample

The XRD patterns of Al 7068−TiC and Al 7068 as a powder sample after 40 h of ball milling are depicted in Fig. 5. The diffraction peaks clearly showed simultaneous broadening and intensity reduction of Al peaks feedback by addition of TiC particles. This issue demonstrated that TiC nanoparticles, acting as milling agent, accelerated the milling process. TiC peaks were detected in diffraction pattern of nanocomposite sample.

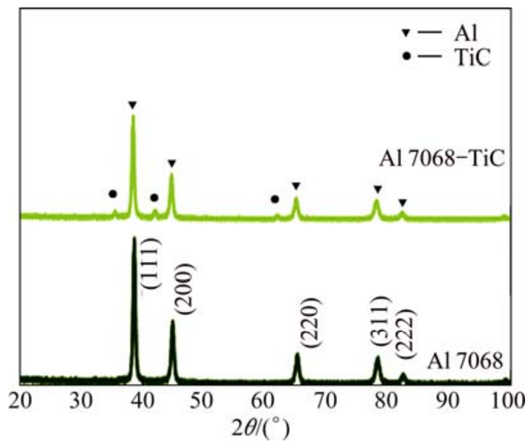

Fig. 5 XRD patterns of Al 7068−PM matrix and Al 7068−TiC nanocomposite

The crystallite size of Al was determined from the broadening of XRD peaks using Williamson–Hall method [37]. The Al crystallite size was refined from 27 to 21 nm by formation of Al matrix nanocomposite at milling time of 40 h. These trends were observed by SIVASANKARAN et al [6] in AA 6061−TiO_2 and KAFTELEN et al [38] in Al_4Cu−TiC composites. Moreover, as observed in Fig. 5, XRD patterns indicated that no detectable interaction layer was identified between TiC and Al alloy matrix (different carbide or intermetallics) during the mixing process.

The effect of reinforcement addition on the morphology of composite powder during mechanical alloying after 40 h is shown in Fig. 6. As it can be seen in this magnified SEM image, nanocomposite particle size was reduced in the presence of TiC nanoparticles. Fracture proceeding of the matrix particles during milling would be accelerated by the addition of hard reinforcement powder due to more collision with balls and more support from hard TiC particles. Therefore, domination of fracture mechanism during milling process resulted in the formation of finer particles. The same result has been reported in Ref. [39].

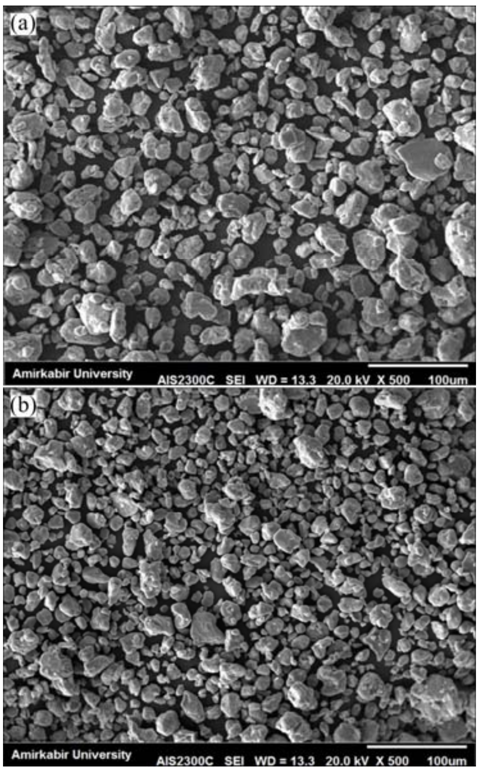

Fig. 6 Variation in morphology of Al 7068−PM (a) and Al 7068−TiC nanocomposite particles (b)

3.2 Optimization of hot pressing process

Al 7068−TiC nanocomposite powder (40 h-milled) was hot-pressed under different conditions obtained by Taguchi method. The layout of orthogonal array to represent the obtained results is shown in Table 2.

Table 2 Conditions and obtained results of test

Test No.	Pressure/MPa	Temperature/°C	Dwelling time/min	Compressive strength/MPa
1	500	440	45	845
2	500	385	30	938
3	500	330	15	611
4	400	440	30	722
5	400	385	15	765
6	400	330	45	553
7	300	440	15	505
8	300	385	45	530
9	300	330	30	461

The results of compression tests and the number of experimental repetitions were applied into Eq. (1) to determine S/N ratio with HB characteristics for each designed condition. These S/N ratio responses for compressive strength results are indicated in Fig. 7. Subsequently, the values of the S/N ratio were substituted into Eq. (2) and then the average of the obtained S/N ratios of a certain factor in the *i*th level, $(M)_{\text{Level}}^{\text{Factor}}$, was calculated (Table 3). Figure 8 shows the mean of S/N ratio for each parameter at three levels for compressive strength. As seen in Fig. 8, three levels of 57.9 (*A*1), 57.2 (*B*2), 56.62 (*C*2) for compressive strength exhibit maximum values of the S/N ratios for factors. According to this designed Taguchi method, simultaneous *A*1, *B*2 and *C*2 hot pressing conditions represent optimum densification requirements to achieve high strength. Meanwhile, the attained outcomes demonstrate that consolidating conditions have a significant impact on the mechanical properties. Based on the obtained results, hot pressing under optimum conditions of 500 MPa, 385 °C and 30 min provides relative density of 98.2 %, high compressive strength of about 938 MPa, and hardness of about HV 265. This indicates that elevating temperature over 385 °C and

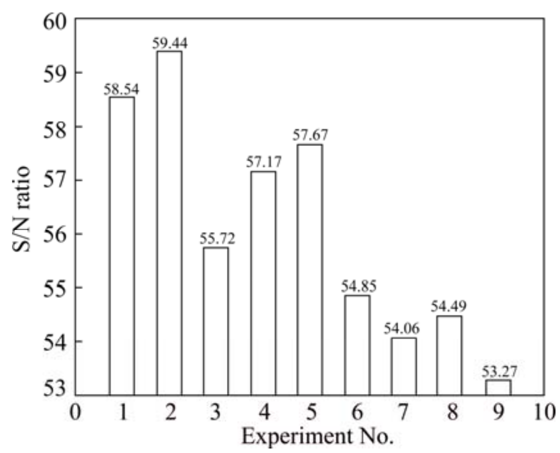

Fig. 7 S/N ratios of samples in tests

Table 3 S/N ratio response of samples

Factor I	Level i	$\left[\left(\frac{S}{N}\right)^{Level}_{Factor}\right]_j$ j=1	j=2	j=3	$(M)^{Level}_{Factor}$
A	1	58.54	59.44	55.72	57.9
A	2	57.17	57.67	54.85	56.56
A	3	54.06	54.49	53.27	53.94
B	1	58.54	57.17	54.06	56.59
B	2	59.44	57.67	54.49	57.2
B	3	55.72	54.85	53.27	54.61
C	1	58.54	54.85	54.49	55.96
C	2	59.44	57.17	53.27	56.62
C	3	55.72	57.67	54.06	55.81

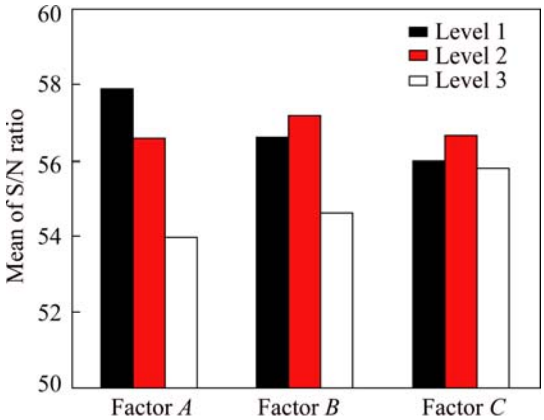

Fig. 8 Means of S/N ratios for each factor

increasing dwelling time for hot pressing process can deteriorate the mechanical properties due to severe grain growth during consolidation.

The results of SEM analysis of Al 7068−TiC nanocomposite consolidated at Taguchi optimal terms are depicted in Fig. 9. As can be seen, $MgZn_2$ phase was identified by SEM analysis of hot pressing 40 h-milled alloy powders (indicated by bold arrows). These particles of additional phase in the matrix were expected to affect the mechanical properties. The same second phase was also observed in similar studies [4]. Meanwhile, it was difficult to determine the difference between the nanometric TiC and micrometric $MgZn_2$ distribution, owning to the limited resolution of SEM.

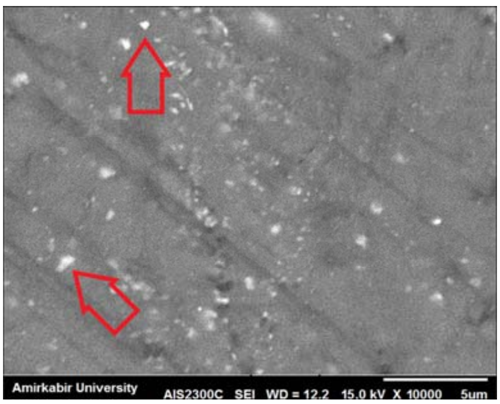

Fig. 9 SEM image of cross section of consolidated sample under optimal conditions

Figure 10 shows the SEM image of the fractured surface for Al 7068−TiC nanocomposite hot-pressed under Taguchi optimal conditions. It can be seen that the specimen presents typical features of ductile fracture. However, some cleavages are found on the fracture surface. Thus, it can be concluded that the sample breaks through combined type of fracture (ductile and brittle), while the composite fails primarily in a brittle manner.

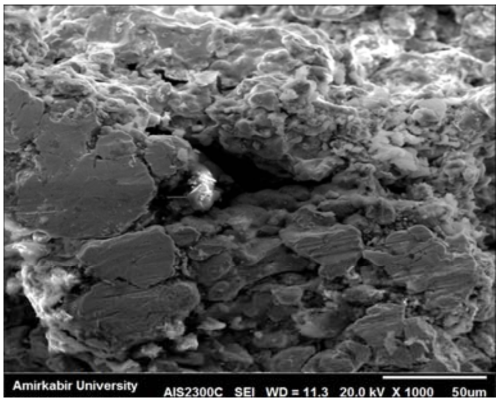

Fig. 10 SEM image for fractured surface of consolidated sample under optimal conditions

Applying the optimal condition for preparing bulk samples from Al alloys in powder form prevents wasting energy during consolidation. To achieve more detailed results, mechanical behavior of samples was examined using a wide range of experiment parameters. For this purpose, two out of three optimal conditions were kept constant and the third parameter was altered.

Figure 11(a) provides data for the compressive strength as function of hot pressing temperature under 500 MPa and 30 min. In other words, Taguchi optimal conditions for pressure and time are kept constant. According to this point graph, mechanical strength is enhanced with increasing compaction temperature, but this trend is reversed by increasing the temperature to higher than 385 °C. Therefore, it can be concluded that severe grain growth is more influential on mechanical properties than densification. The next important issue to be considered is that what happens with increasing the pressure to higher than 500 MPa. Figure 11(b) shows compressive strength as a function of compaction pressure at 385 °C for 30 min (Taguchi optimal terms which are kept constant). As can be seen in the related graph, the maximum strength is enhanced with the reduced rate by increasing the applied pressure. It can be also observed that this strength increment is inconsiderable when pressure increases to higher than

500 MPa. FOGAGNOLO et al [40] previously reported the similar results for Al 6061 alloy. Moreover, declining rate of increasing relative density versus hot pressing pressure is decipherable from the Panelli and Ambrosio Filho equation [41].

Figure 12 shows an arbitrary illustration of the polished cross-sectional area of samples under different consolidation conditions by OM. The effect of low exposed temperature (250 °C) on microstructures is depicted in Fig. 12(a) which is under optimum pressure and adequate time. As can be observed, low temperature results in development of fine porosity with size ranging from 100 nm to 5 μm within compacted samples. Fine and spherical shape of pores as effect of low temperature can strongly increase crack-growth. Figure 12(b) indicates the effect of low applied pressure (300 MPa) on the shape and size of formed porosity. Using poor hot pressing pressure leads to creation of non-uniform larger cavities than low temperature state. In addition, the OM image of consolidated sample in both low temperature and pressure (250 °C and 300 MPa) is shown in Fig. 12(c). Large congested pores are outcomes of compaction under defined condition and this shows high degrees of defects. It is proved that these defects are destructive for load bearing of samples as they are stress concentration points. Large volume fraction of porosities (more than 15%) was obtained considering poor consolidation conditions. Finally, the illustration of hot-

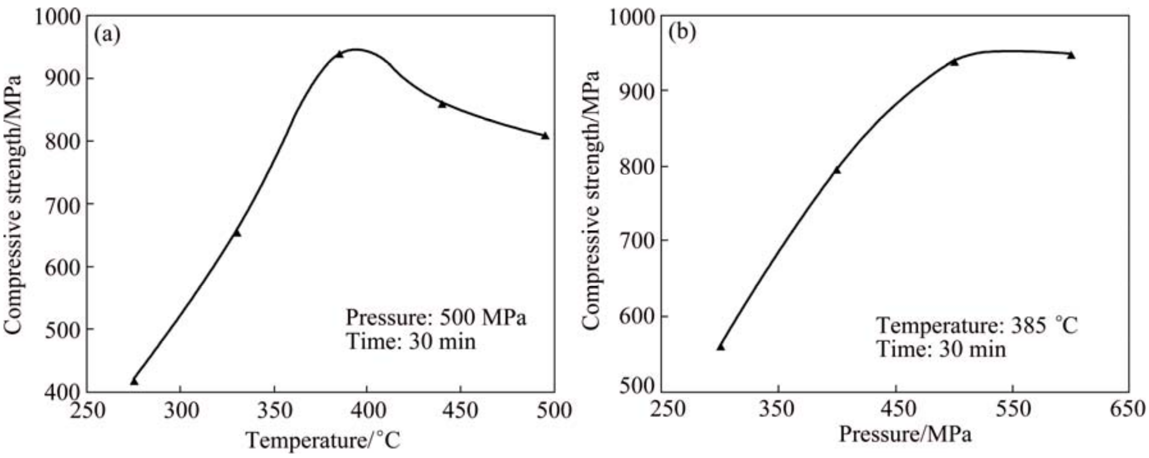

Fig. 11 Compressive strength of hot-pressed samples at different applied temperatures (a) and pressures (b)

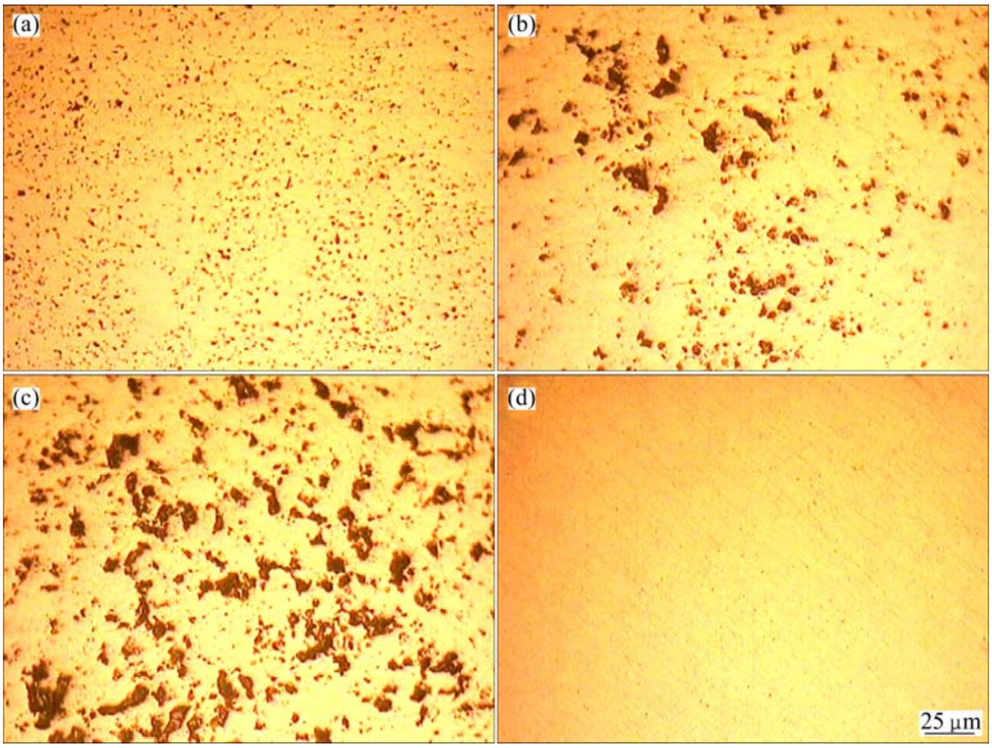

Fig. 12 OM images of samples produced under hot pressing conditions of 250 °C, 500 MPa (a), 385 °C, 300 MPa (b), 250 °C, 300 MPa (c) and 385 °C, 500 MPa (d)

pressed sample under optimal Taguchi conditions (Fig. 12(d)) represents high density and evenness. The volume fraction of porosities for optimal Taguchi conditions is less than 1.5% which represents high density sample by hot pressing method.

3.3 Analysis of variance (ANOVA)

Mathematics assessment to analyze the contribution percentage of each controllable factor was carried out using the analysis of variance. Initially, the mean magnitude of the measurement outcomes of a specified factor in the kth level ($\overline{Y}_k^{\mathrm{F}}$) was achieved from Y_i and determined values are listed in Table 4. The factorial sum of squares, $\mathrm{SS_F}$, for each factor was computed exclusively with pasting $\overline{Y}_k^{\mathrm{F}}$ and $\overline{Y}_\mathrm{T}$ =658.89 into Eq. (5). In the next step, the total sum of squares ($\mathrm{SS_T}$) was calculated by Eq. (4). The variance of error (V_Er) was resulted from entering $\mathrm{SS_F}$ and $\mathrm{SS_T}$ =662189.13 in Eq. (6). Ultimately, the contribution percentage of each controllable factor (ρ_F) was estimated consecutively by substitution of $\mathrm{SS_F}$, $\mathrm{SS_T}$, V_Er=1161.024, and $\mathrm{DOF_F}$ =2 in Eq. (3). Figure 13 shows obtained results for significance of hot pressing controllable factors. The rank order of the contributions percentage of each factor in hot pressing terms is as follows: 1) applied pressure (61.3%), 2) exposed temperature (29.53%), 3) dwelling hot pressing time (4.49%). Thus, the contribution percentage of error is 4.68%, which is tolerable value for Taguchi approach. According to their values, the employed hot pressing pressure is most effective term to get higher compression strength. It is important to note that the percentage results were obtained for defined limits for pressure, temperature and time, which were chosen considering recent works in this field to make the results rational.

Table 4 $\overline{Y}_k^{\mathrm{F}}$ table for analysis of variance

Level	$\overline{Y}_k^A$	$\overline{Y}_k^B$	$\overline{Y}_k^C$
1	798	690.67	642.67
2	680	744.33	707
3	498.67	541.67	627

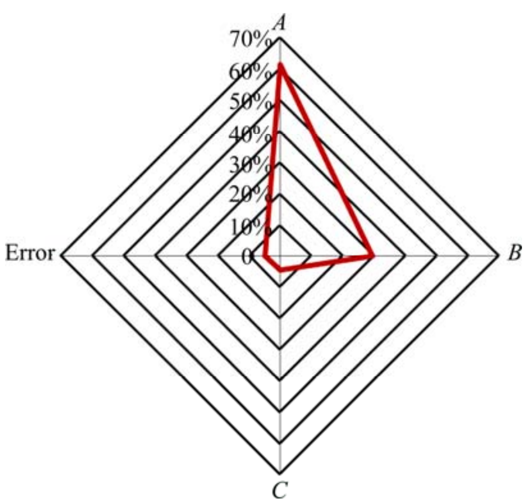

Fig. 13 Contribution percentage of each hot pressing factor

4 Conclusions

1) Al 7068−5%TiC nanocomposite powder was synthesized by mechanical alloying after 40 h milling of initial elemental powders and TiC nanoparticles. Broadening and intensity reduction of Al XRD peaks of nanocomposite in comparison with matrix indicated Al crystallite refinement with addition of TiC as reinforcement. Moreover, no interaction layer was identified between TiC and Al alloy matrix (different carbide or intermetallics) during the milling by XRD patterns. Nanocomposite sample possesses finer particles than unreinforced matrix due to the fact that fracture mechanism of the particles during milling was accelerated by adding hard TiC reinforcement.

2) According to Taguchi experimental design approach, hot pressing under 500 MPa, 385 °C and 30 min provided relative density of 98.2% and high compressive strength and hardness about 938 MPa and HV 265, respectively. Extra experiment results confirmed that higher pressure had no considerable effect on mechanical properties and further increase in temperature had reverse effect due to severe grain growth.

3) The contribution percentage achievement of controllable terms was determined by analysis of variance. The applied compaction pressure is the most effective term (about 61.3%) to obtain higher compression strength.

References

[1] PALMEAR I J. Light alloys: From traditional alloys to nanocrystals [M]. 4th ed. Amsterdam: Elsevier, 2006.

[2] LI Yuan-yuan, ZHENG Xiao-ping, ZHANG Wei-wen, LUO Zong-qiang. Effect of deformation temperature on microstructures and properties of 7075/6009 alloy [J]. Transactions of Nonferrous Metals Society of China, 2009, 19(5): 1037−1043.

[3] AZIMI A, FALLAHDOOST H, NEJADSEYFI O. Microstructure, mechanical and tribological behavior of hot-pressed mechanically alloyed Al−Zn−Mg−Cu powders [J]. Materials and Design, 2015, 75: 1−8.

[4] AZIMI A, SHOKUHFAR A, ZOLRIASATEIN A. Nanostructured Al−Zn−Mg−Cu−Zr alloy prepared by mechanical alloying followed by hot pressing [J]. Materials Science and Engineering A, 2014, 595: 124−130.

[5] YAZDIAN N, KARIMZADEH F, TAVOOSI M. Microstructural evolution of nanostructure 7075 aluminum alloy during isothermal annealing [J]. Journal of Alloys and Compounds, 2010, 493: 137−141.

[6] SIVASANKARAN S, SIVAPRASAD K, NARAYANASAMY R, IYER V K. An investigation on flowability and compressibility of AA 6061_{100-x}−x wt.% TiO_2 micro and nanocomposite powder

prepared by blending and mechanical alloying prepared by blending and mechanical alloying [J]. Powder Technology, 2010, 201: 70−82.

[7] VAROL T, CANAKCI A. Effect of weight percentage and particle size of B_4C reinforcement on physical and mechanical properties of powder metallurgy Al 2024−B_4C composites [J]. Metals and Materials International, 2013, 9: 1227−1234.

[8] KHOSRAVI H, BAKHSHI H, SALAHINEJAD E. Effects of compocasting process parameters on Microstructural characteristics and tensile properties of A356−SiC_p composites [J]. Transactions of Nonferrous Metals Society of China, 2014, 24(8): 2482−2488.

[9] MOGHADAM A D, OMRANI E, MENEZES P L, ROHATGI P K. Mechanical and tribological properties of self-lubricating metal matrix nanocomposites reinforced by carbon nanotubes (CNTs) and grapheme—A review [J]. Composites Part B, 2015, 77: 402−420.

[10] SURYANARAYANA C. Mechanical alloying and milling [J]. Progress in Materials Science, 2001, 46: 1−184.

[11] KURSUN C, GOGEBAKAN M. Characterization of nanostructured Mg−Cu−Ni powders prepared by mechanical alloying [J]. Journal of Alloys and Compounds, 2015, 619: 138−144.

[12] GOGEBAKAN M, KURSUN C, ECKERT J. Formation of new Cu-based nanocrystalline powders by mechanical alloying technique [J]. Powder Technology, 2013, 247: 172−177.

[13] PARVIN N, ASSADIFARD R, SAFARZADEH P, SHEIBANI S, MARASHI P. Preparation and mechanical properties of SiC-reinforced Al 6061 composite by mechanical alloying [J]. Materials Science and Engineering A, 2008, 492: 134−140.

[14] TAVOOSI M, KARIMZADEH F, ENAYATI M H, HEIDARPOUR A. Bulk Al−Zn/Al_2O_3 nanocomposite prepared by reactive milling and hot pressing methods [J]. Journal of Alloys and Compounds, 2009, 475: 198−201.

[15] POIRIER D, DREW R A L, TRUDEAU M L, GAUVIN R. Fabrication and properties of mechanically milled alumina/aluminum nanocomposites [J]. Materials Science and Engineering A, 2010, 527: 7605−7614.

[16] JAFARI M, ABBASI M H, ENAYATI M H, KARIMZADEH F. Mechanical properties of nanostructured Al 2024−MWCNT composite prepared by optimized mechanical milling and hot pressing methods [J]. Advanced Powder Technology, 2012, 23: 205−210.

[17] ATRIAN A, MAJZOOBI G H, ENAYATI M H, BAKHTIARI H. A comparative study on hot dynamic compaction and quasi-static hot pressing of Al7075/SiCnp nanocomposite [J]. Advanced Powder Technology, 2015, 26: 73−82.

[18] ZEBARJAD S M, SAJJADI S A. Microstructure evaluation of Al−Al_2O_3 composite produced by mechanical alloying method [J]. Materials and Design, 2006, 27: 684−688.

[19] ZHANG D L, KOCH C C, SCATTERGOOD R O. The role of new particle surfaces in synthesizing bulk nanostructured metallic materials by powder metallurgy [J]. Materials Science and Engineering A, 2009, 516: 270−275.

[20] GALANTY M, KAZANOWSKI P, KANSUWAN P, MISIOLEK W Z. Consolidation of metal powders during the extrusion process [J]. Journal of Materials Processing Technology, 2002, 125−126: 491−496.

[21] VAROL T, CANAKCI A, OZSAHIN S. Prediction of the influence of processing parameters on synthesis of Al 2024−B_4C composite powders in a planetary mill using an artificial neural network [J]. Science and Engineering of Composite Materials, 2014, 21: 411−420.

[22] CANAKCI A, OZSAHIN S, VAROL T. Prediction of effect of reinforcement size and volume fraction on the abrasive wear behavior of AA 2014/B_4C_p MMCs using artificial neural network [J]. Arabian Journal for Science and Engineering, 2014, 39: 6351−6361.

[23] CANAKCI A, ERDEMIR F, VAROL T, PATIR A. Determining the effect of process parameters on particle size in mechanical milling using the Taguchi method: Measurement and analysis [J]. Measurement, 2013, 46: 3532−3540.

[24] CANAKCI A, VAROL T, OZSAHIN S. Analysis of the effect of a new process control agent technique on the mechanical milling process using a neural network model: Measurement and modeling [J]. Measurement, 2013, 46: 1818−1827.

[25] KRASNOWSKI M, KULIK T. Nanocrystalline FeAl intermetallic produced by mechanical alloying followed by hot-pressing consolidation [J]. Intermetallics, 2007, 15: 201−205.

[26] KRASNOWSKI M, KULIK T. Nanocrystalline FeAl matrix composites reinforced with TiC obtained by hot-pressing consolidation of mechanically alloyed powders [J]. Intermetallics, 2007, 15: 1377−1383.

[27] KRASNOWSKI M, KULIK T. Nanocrystalline Al−Fe intermetallics — Light weight alloys with high hardness [J]. Intermetallics, 2010, 18: 47−50.

[28] AZIMI A, SHOKUHFAR A, NEJADSEYFI O. Mechanically alloyed Al 7075−TiC nanocomposite: Powder processing, consolidation and mechanical strength [J]. Materials and Design, 2015, 66: 137−141.

[29] CANAKCI A, VAROL T. Microstructure and properties of AA 7075/Al−SiC composites fabricated using powder metallurgy and hot pressing [J]. Powder Technology, 2014, 268: 72−79.

[30] RAJMOHAN T, PALANIKUMAR K, KATHIRVEL M. Optimization of machining parameters in drilling hybrid aluminium metal matrix composites [J]. Transactions of Nonferrous Metals Society of China, 2012, 22(6): 1286−1297.

[31] SALEHI M, SAADATMAND M, AGHAZADEH MOHANDESI J. Optimization of process parameters for producing AA 6061/SiC nanocomposites by friction stir processing [J]. Transactions of Nonferrous Metals Society of China, 2012, 22(5): 1055−1063.

[32] TAGUCHI G. Introduction to quality engineering [M]. New York: McGraw-Hill, 1990.

[33] CHOU C, LIN S, PENG C, LU W. The optimum conditions for preparing solid fuel briquette of rice straw by a piston-mold process using the Taguchi method [J]. Fuel Processing Technology, 2009, 90: 1041−1046.

[34] SCHATT W, WIETERS K P. Powder metallurgy: processing and materials [M]. Shrewsbury: European Powder Metallurgy Association, 1997.

[35] VAROL T, CANAKCI A. Effect of particle size and ratio of B_4C reinforcement on properties and morphology of nanocrystalline Al 2024−B_4C composite powders [J]. Powder Technology, 2013, 246: 462−472.

[36] CANAKCI A, VAROL T. Structural evolution and characterization of nanostructured Al−Al_2O_3 composite fabricated by mechanical alloying method [J]. Romanian Journal of Materials, 2013, 43: 312−319.

[37] WILLIAMSON G K, HALL W H. X-ray line broadening from filed aluminum and wolfram [J]. Acta Metallurgica, 1953, 1: 22−31.

[38] KAFTELEN H, UNLU N, GÖLLER G, ÖVECOĞLU M L, HENEIN H. Comparative processing–structure–property studies of Al−Cu matrix composites reinforced with TiC particulates [J]. Composites Part A, 2011, 42: 812−824.

[39] JABBARI TALEGHANI M A, RUIZ NAVAS E M, TORRALBA J M. Microstructural and mechanical characterisation of 7075 aluminium alloy consolidated from a premixed powder by cold compaction and hot extrusion [J]. Materials and Design, 2014, 55: 674−682.

[40] FOGAGNOLO J B, ROBERT M H, TORRALBA J M. Mechanically alloyed AlN particle-reinforced Al−6061 matrix composites: Powder processing, consolidation and mechanical strength and hardness of the as-extruded materials [J]. Materials Science and Engineering A, 2006, 426: 85−94.

[41] PANELLI R, AMBROSIO FILHO F. A study of a new phenomenological compacting equation [J]. Powder Technology, 2001, 114: 255−261.

Taguchi 统计学分析方法优化 Al 7068−TiC 纳米复合材料的凝固行为

Amin AZIMI[1], Ali SHOKUHFAR[2,3], Omid NEJADSEYFI[2], Hamid FALLAHDOOST[2], Saeid SALEHI[3]

1. Young Researchers and Elite Club, South Tehran Branch, Islamic Azad University, Tehran, Iran;
2. Advanced Materials and Nanotechnology Research Center, Department of Mechanical Engineering, K. N. Toosi University of Technology, Tehran, Iran;
3. Department of Engineering, Karaj Branch, Islamic Azad University, Karaj, Iran

摘 要：采用机械合金化和热压工艺制备高强 Al 7068−5%TiC(质量分数)纳米复合材料。基于致密化的重要性和晶粒生长的影响，以获得较高抗压强度为目标，采用 Taguchi 统计法对制备 Al 7068−5%TiC 块体纳米复合材料的热压条件进行优化。结果表明：在 500 MPa 和 385 °C 下热压 30 min 能获得抗压强度为 938 MPa、硬度为 HV 265 的 Al 7068−TiC 纳米复合材料。此外，方差分析结果表明，外加压力是影响纳米复合材料热压过程最关键的因素。各因素对纳米复合材料热压过程影响贡献率为外加压力(61.3%)、热压温度(29.53%)和热压时间(4.49%)。

关键词：Al 7068−TiC 纳米复合材料；热压处理；机械合金化；Taguchi 法；力学性能

(Edited by Wei-ping CHEN)